

Dynamical behavior of a new jerk system inspired from chaotic memory oscillators

Saad Fawzi AL-AZZAWI 

This paper constructs a six-term new simple 3D jerk system modeled by chaotic model memory oscillators with four parameters that control the behavior. The suitable choice of one of these parameters helps the system describe behavior and attractors. This means that the choice is a parameter of the associated behavior (dissipative or conservative) and attractors (self-excited or hidden). Some features of the equilibrium are observed that are related to the dependence on these parameters, such as saddle-foci, non-hyperbolic, and node-foci. This system is rich in dynamic features including chaotic, quasi-periodic (2-torus), and periodic via the utilization of bifurcation diagrams and Lyapunov spectrum. Finally, a new image encryption algorithm is introduced that utilizes the jerk system. The algorithm is assessed through statistical performance analysis, according to the results of the experiments and security tests, it has been verified that the suggested image encryption algorithm is highly secure and could be a viable option for real-world applications.

Key words: chaotic memory oscillators (MO_4), jerk system, elegant system, encryption, decryption

1. Introduction

Chaotic systems are dynamical systems that exhibit sensitive dependence on initial conditions, meaning that small changes in the initial conditions can lead to vastly different outcomes. One important feature of chaotic systems is that their behavior can be influenced by parameter (coefficient) values. In particular, a system may exhibit chaotic behavior only within a certain range of parameter values, beyond which it may converge to a stable state or exhibits periodic behavior as in the Lorenz system [1], which exhibits chaotic and stable behavior relying on one of its parameters [2].

Copyright © 2024. The Author(s). This is an open-access article distributed under the terms of the Creative Commons Attribution-NonCommercial-NoDerivatives License (CC BY-NC-ND 4.0 <https://creativecommons.org/licenses/by-nc-nd/4.0/>), which permits use, distribution, and reproduction in any medium, provided that the article is properly cited, the use is non-commercial, and no modifications or adaptations are made

S.F. Al-Azzawi (e-mail: saad_alazawi@uomosul.edu.iq) is with Department of Mathematics, College of Computer Science and Mathematics, University of Mosul, Mosul, Iraq.

Received 1.08.2023. Revised 7.12.2023.

In 1994, Sprott identified 19 different chaotic systems, labeled A through S [3]. These systems are simpler than the Lorenz model because they only consist of five or six terms. Most of these systems are referred to as “elegant systems” [4,5] because they have most parameters (coefficients) that are set to zero, with the rest parameters being either ± 1 , a decimal fraction, or a small integer. Sprott used these special coefficients looking for cases for which the first Lyapunov exponent exceeds the threshold of 0.001 that are required to identify chaos. However, it should be noted that any system without parameters produces special cases. Therefore, the parameters play a crucial role in the analysis and study of the behavior of systems. Researchers have extensively utilized these systems to generate high-dimension systems with a fewer number of terms [6–13].

Any dynamical system is composed of a set of variables and parameters. Understanding the role of each parameter in a system, many mathematical systems can be created that accurately predict its behavior in different scenarios: state feedback control and coupling strategy [14–16]. One important application of parameter analysis is in the field of electronic circuits via NI Multisim to identify the optimal resistors and capacitors that will achieve the desired performance characteristics [17–19]. The problem of stabilization for delay fuzzy systems with parameters to an estimated controller of the nonlinear Takagi-Sugeno parameterized systems [20]. Overall, the study of parameters is essential for explaining the behavior of systems in various fields.

In 2010, Sprott [5] identified 16 chaotic model memory oscillators (MO_i) which are called $MO_0, MO_1, MO_2, \dots, MO_{15}$. It is clear that all these models are homogeneous third-order explicit ordinary differential equations (3rd ODEs) with single variable x , also called a jerk equation $\ddot{x} = J(x, \dot{x}, \ddot{x})$, where the first derivative represents velocity, the second derivative represents acceleration, and the third derivative represents *jerk*. Memory oscillators are a class of dynamical systems that exhibit interesting and complex behavior and can be recast in the form of systems that consist of a set of first-order differential equations. According to [17], these memory oscillator models are special cases of the more general class of chaotic electrical circuit

$$\ddot{x} + A\dot{x} + \dot{x} - G(x) = 0. \quad (1)$$

A is constant, $G(x)$ – nonlinear function (nonlinear feedback element) as shown in Fig. 1.

Several 3D ordinary differential equation (ODE) systems have been adopted based on the jerk equation and Sprott’s criteria for constructing a new chaotic systems [21]. These systems focus on a limited number of terms and an indefinite number of quadratic nonlinearities. In 2013, Molaie et al. [4] identified six chaotic jerk systems (SE_1 – SE_6) with node-foci equilibria, which were deemed “simple

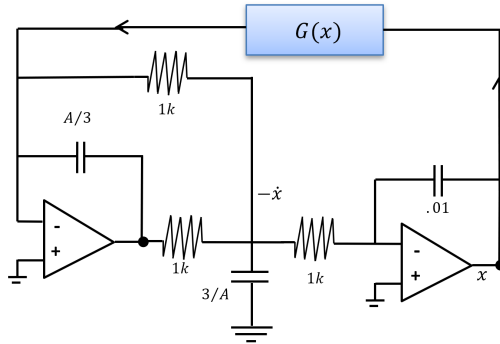


Figure 1: A general chaotic electrical circuit [17]

systems” at that time due to their composition of seven or eight terms as per [4]. In 2015, another jerk system derived from memory oscillators MO_{11} was presented, which was deemed simpler than SE_1, \dots, SE_6 systems as it included only six terms with specific coefficients [22]. In 2017, Vaidyanathan et al. [23] introduced a jerk system composed of seven terms and five parameters. Similar to conventional systems, these parameters played a significant role in influencing the chaotic behavior. However, the other parameters did not influence the dynamic properties of the system except for one parameter related to divergence [23].

Recently, there has been significant attention from researchers towards jerk systems, due to their potential applications in diverse fields including image encryption [24, 25] and optimization [26]. Several studies have been conducted on different types of jerk systems, and Table 1 provides a comprehensive summary and offers detailed information on various jerk systems of these studies organized by publication year. For instance, in 2018, publications such as [27–29] were released, followed by [30] in 2019, [31–34] in 2020, [35–38] in 2021, and [39–41] in 2022. Newly, Vaidyanathan et al. introduced a new 3D jerk system with eight terms and three parameters in 2022 [42]. It is clear from Table 1 that most parameters of the systems played a minor role in analyzing and investigating the characteristics of each system.

Until now, chaotic behavior is still important in various systems, such as the chaotic Colpitts oscillator [43]. This paper focuses on introducing a new chaotic oscillator with a triangular wave non-linearity. Additionally, a 3D chaotic biology system, comprising one prey and two predators, is presented [44]. Another study introduces a new 3D chaotic Thomas’ system, where a fractional derivative (specifically, Riemann-Liouville) is utilized to gain a better understanding of the system’s dynamics [45]. The researchers thoroughly examine the system for different fractional index values to demonstrate the sensitivity of chaotic systems

Table 1: Some of the reported chaotic jerk models with active parameters

No.	Refs.		Total no. of terms	Nonlinearities and their type		No. of parameters	No. of active parameters
				No. of nonlinear	Type		
1-6	[4], 2013 six models	SE ₁	7	2	Quadratic, Cross product	without parameters	-
		SE ₂	8	3			
		SE ₃	7	2			
		SE ₄	7	2			
		SE ₅	7	2			
		SE ₆	7	3			
7	[21], 2015	6	2	Two Exponentials	2	1	
8	[22], 2017	7	3	Cross product, Cubic	5	1	
9	[26], 2018	6	2	Two Exponentials	4	2	
10	[27], 2018	7	3	Quadratic, Cross product	7	1	
11	[28], 2018	6	1	Cubic	6	3	
12	[29], 2019	6	1	Exponential	2	2	
13	[30], 2019	7	2	Quadratic, Cross product	3	3	
14	[31], 2020	7	3	Quadratic, Cross product, Cubic	3	1	
15	[32], 2020	7	2	Quadratic, Cubic	4	3	
16	[33], 2020	6	1	Sine hyperbolic function	3	2	
17	[34], 2020	8	3	Quadratic, Cross product	8	3	
18	[35], 2021	6	1	Cubic	4	1	
19	[36], 2021	7	2	Quadratic, Cross product	2	1	
20	[37], 2021	7	2	Quadratic, Cross product	2	-	
21	[38], 2021	7	2	Quadratic, Cross product	4	1	
22	[39], 2022	6	1	Cubic	2	2	
23	[40], 2022	7	1	Sine hyperbolic function	5	2	
24	[41], 2022	7	2	Quadratic, Cross product	4	1	
25	[42], 2022	8	3	Quadratic, Cross product	3	3	
26	This work	6	2	Quadratic, Exponential	4	4 (all)	

to initial conditions. In a different study, a speech cryptosystem based on the 3D new chaotic system is proposed a speech cryptosystem based on the 3D new chaotic system [46]. However, there have been many previous studies on chaotic systems and oscillators. This motivated us to propose a new six-term jerk system with four parameters, inspired by chaotic memory oscillators, where each parameter has a significance on the proposed system.

In the following points, the exceptional and captivating attributes of the proposed system will be outlined.

- The proposed system is relatively simple compared to other systems of a similar nature in existing literature, as it contains only one exponential term and four parameters among its total of six terms.
- Every parameter plays a significant role in the evaluation of the proposed system's dynamics:
 - (i) The determination of stability is affected by the crucial parameters a_1 and a_3 .
 - (ii) The system's dynamics are influenced by the bifurcation parameter a_2 , and it can exhibit different behavior such as periodic, quasi-periodic (2-torus), and chaotic behavior.
 - (iii) The classification of this system as either dissipative or conservative is determined by the divergence analysis, which is based on the parameter a_3 .
 - (iv) Parameter a_4 plays a crucial role in determining whether attractors are self-excited or hidden based on equilibria.
- A new algorithm for encrypting images is proposed, which involves utilizing the jerk system. The algorithm's security is tested, and its effectiveness is evaluated.

2. A new 3D jerk system

Let us recall the fifth class MO_4 [6] which includes a quadratic polynomial i.e.,

$$\ddot{x} + 0.5\dot{x} + \dot{x} - \underbrace{x(x-1)}_{G(x)} = 0. \quad (2)$$

It is convenient to convert the ODE (2) in a 3-D system having six terms by setting $y = \dot{x}$, $z = \ddot{x}$ i.e.,

$$\begin{cases} \dot{x} = y, \\ \dot{y} = z, \\ \dot{z} = -x - y - 0.5z + x^2. \end{cases} \quad (3)$$

System (3) can be expressed in a general form via the equivalent system as

$$\begin{cases} \dot{x} = y, \\ \dot{y} = z, \\ \dot{z} = a_1x + a_2y + a_3z + a_4x^2. \end{cases} \quad (4)$$

In which $a_1 = a_2 = 1$, $a_3 = -0.5$, and $a_4 = 1$. According to parameters (coefficients) a_i , system (4) is categorized into elegant [4, 5] or no elegant jerk model as:

The system (4) can be classified as an elegant or non-elegant jerk model based on its parameters, as indicated by the value of a_i :

- Elegant system if many $a_i = \pm 1/0$ or other $a_i < 1$ (decimal fraction or small integer).
- No elegant system if many $a_i \neq \pm 1/0$ or other $a_i > 1$ (greater than one).

The classification of the system (4) as an elegant or non-elegant jerk model depends on the values of its parameters, specifically the value of a_i . If the majority of a_i values are either equal to $\pm 1/0$ or less than 1 (represented as a decimal fraction or small integer), then the system is considered an elegant one. On the other hand, if the majority of a_i values are not equal to $\pm 1/0$ or greater than 1, then the system is classified as a non-elegant one. Such system (4) is called jerk system and the general form of jerk equation as

$$J(x, y, z) = a_1x + a_2y + a_3z + a_4x^2 + a_5y^2 + a_6z^2 + a_7xy + a_8xz + a_9yz + a_{10}, \quad (5)$$

where

$$J(x, y, z) = \ddot{x} = J(x, \dot{x}, \ddot{x}) \quad (6)$$

and the third derivative of the system (6) i.e., $\ddot{x} = \frac{d^3x}{dx^3} = \dot{x}_3$ represents the jerk. So, the MO_4 model belongs to the family of jerk systems.

Relying on the model (3) and Eq. (5), a new simple jerk model inspired by MO_4 is proposed which can be depicted as:

$$\begin{cases} \dot{x} = y, \\ \dot{y} = z, \\ \dot{z} = -a_1x - a_2e^y - a_3z + a_4x^2, \end{cases} \quad (7)$$

where a_i , $i = 1, \dots, 4$ are control parameters and by adjusting these parameters, it is possible to obtain various types of peculiar attractors. System (7) has chaotic behavior under typical $(a_1, a_2, a_3, a_4) = (3, 0.25, 11.5, 1)$ with initial conditions $(0, 0.1, 0)$ as shown in Fig. 2a. It is clear that both the MO_4 system (3) and a new jerk system (7) have six terms, but with replaced the linear term $(-y)$ in the third ODE of (3) with exponential nonlinear term $(-e^y)$ in the proposed system.

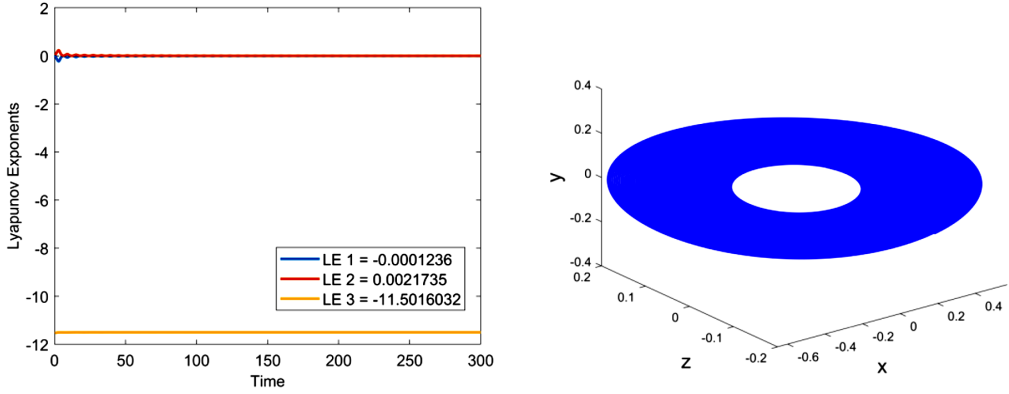


Figure 2: Lyapunov exponents and chaotic attractor for the new system

3. Dynamical analysis of the jerk system

3.1. Dissipativity and conservative

These two properties are essential for understanding the dynamical behavior of this jerk system and how it can be used for various applications. The dissipative nature of this system ensures that it does not lose energy over time, while the conservative nature ensures that its momentum is preserved. By studying these properties, we can gain insight into how this new jerk system behaves in different circumstances and what kind of applications it could be useful for.

The divergence of the system (7) can be obtained as

$$\nabla V = \frac{\partial \dot{x}}{\partial x} + \frac{\partial \dot{y}}{\partial y} + \frac{\partial \dot{z}}{\partial z} = -a_3. \quad (8)$$

Note that the divergence based on control parameter a_3 only as:

- If $a_3 > 0$, then the system is dissipative,
- If $a_3 = 0$, then the system is conservative,
- If $a_3 < 0$, then the system is unbounded.

3.2. Lyapunov exponents and Lyapunov dimension

System (7) has one positive Lyapunov exponent under $(a_1, a_2, a_3, a_4) = (3, 0.25, 11.5, 1)$ with initial condition $(0, 0.1, 0)$ as depicted in Fig. 2 as follows

$$\begin{cases} \text{LE}_1 = 0.0022, \\ \text{LE}_2 = -\mathbf{0.0001} \approx 0, \\ \text{LE}_3 = -11.5016, \end{cases} \quad \sum_{i=1}^3 \text{LE}_i = -11.4996, \quad (9)$$

whereas, the Lyapunov dimension (D_L) given as

$$D_L = j + \frac{1}{|LE_{j+1}|} \sum_{i=1}^j LE_i \implies D_L = 2 + \frac{0.0022 - 0.0001}{|LE_3|} = 2.0002. \quad (10)$$

The degree to which a system exhibits chaotic behavior may be measured using the Lyapunov dimension.

3.3. Equilibria and stability

System (7) categories as hidden and self-excited attractors relying on parameter a_4 as:

- If $a_4 = 0$, then the system (7) is without equilibria and belongs to hidden attractors.
- If $a_4 \neq 0$, then the system (7) has two unstable equilibria and belongs to self-excited attractors.

Under $a_4 \neq 0$, system (7) has equilibria $E_{1,2} = \left(\frac{a_1 \pm \sqrt{a_1^2 + 4a_2a_4}}{2a_4}, 0, 0 \right)$ and it

can be written in a general form as $E(x^*, 0, 0)$ where $x^* = \frac{a_1 \pm \sqrt{a_1^2 + 4a_2a_4}}{2a_4}$.

The Jacobian and the corresponding characteristic polynomial are given in Eq. (11) and Eq. (12), respectively.

$$J = \begin{bmatrix} 0 & 1 & 0 \\ 0 & 0 & 1 \\ -a_1 + 2a_4x & -a_2e^y & -a_3 \end{bmatrix} \xrightarrow{J(E_{1,2})} \begin{bmatrix} 0 & 1 & 0 \\ 0 & 0 & 1 \\ \pm\sqrt{a_1^2 + 4a_2a_4} & -a_2 & -a_3 \end{bmatrix} \quad (11)$$

$$E_1: \quad p(\lambda) = \lambda^3 + a_3\lambda^2 + a_2\lambda - \sqrt{a_1^2 + 4a_2a_4}, \quad (12a)$$

$$E_2: \quad p(\lambda) = \lambda^3 + a_3\lambda^2 + a_2\lambda + \sqrt{a_1^2 + 4a_2a_4}. \quad (12b)$$

The system (7) is always unstable at point E_1 due to the final term of Eq. (12a) is negative. Therefore, the investigation for stability at point E_2 is considered only to check whether it is stable or not. Now, the Hurwitz matrix of the above equation

at E_2 as

$$H = \begin{bmatrix} a_3 & \sqrt{a_1^2 + 4a_2a_4} & 0 \\ 1 & a_2 & 0 \\ 0 & a_3 & \sqrt{a_1^2 + 4a_2a_4} \end{bmatrix}.$$

Based on the Routh -Hurwitz criterion, constraints are required as

- $\Delta_1 = |a_3| > 0,$
- $\Delta_2 = \begin{vmatrix} a_3 & \sqrt{a_1^2 + 4a_2a_4} \\ 1 & a_2 \end{vmatrix} = a_2a_3 - \sqrt{a_1^2 + 4a_2a_4} > 0,$
- $\Delta_3 = \sqrt{a_1^2 + 4a_2a_4}, \quad \Delta_2 > 0.$

Consequently, the Eq. (12b) has three eigenvalues with negative real part at the next conditions:

$$a_3 > 0, \quad a_1 > \sqrt{a_2(a_2a_3^2 - 4a_4)} = a_C. \quad (13)$$

If $a_1 = a_C$, then it is termed a critical value.

Corollary 1. (Critical Value) *The jerk system has a critical value at the equilibrium E_2 as*

$$a_1 = a_C = \sqrt{a_2(a_2a_3^2 - 4a_4)}. \quad (14)$$

Proof. Hopf bifurcation for Eq. (12b) occur of the transit via the coefficients $a_3a_2 - \sqrt{a_1^2 + 4a_2a_4} = 0 \Rightarrow (a_3a_2)^2 = a_1^2 + 4a_2a_4 \Rightarrow a_1 = \sqrt{a_2(a_2a_3^2 - 4a_4)} = a_C.$

Corollary 2. *Under condition (14), Eq. (12b) has one pair of pure-imaginary roots, and the solutions are $\lambda_1 = -a_3, \lambda_{2,3} = \pm\sqrt{a_2}i.$*

Proof. Let $\lambda_{2,3} = \pm bi$ be the complex solutions and λ_1 the real solution of Eq. (12b) then, utilize the law $\lambda_1 + \lambda_2 + \lambda_3 = -a_3 \rightarrow \lambda_1 = -a_3.$ This readily leads to $a_3 > 0, a_1 = \sqrt{a_2(a_2a_3^2 - 4a_4)}$ and $\lambda_1 = -a_3, \lambda_{2,3} = \pm\sqrt{a_2}i.$ So, system (7) exhibits a Hopf bifurcation at the point $E_2.$ Consequently, the point E_2 loses its stability at $a_1 = a_C.$

Theorem 1. *If $a_1 = \sqrt{a_2(a_2a_3^2 - 4a_4)},$ Eq. (12b) has a negative eigenvalue $\lambda_1 = -a_3 < 0$ together with one pair of pure-imaginary eigenvalues $\lambda_{2,3} = \pm\sqrt{a_2}i$ such that $\text{Re}(\lambda'(a_C)) \neq 0,$ therefore the system (7) exhibits a Hopf bifurcation at the point $E_2.$*

Proof. If $a_1 = a_C = \sqrt{a_2(a_2a_3^2 - 4a_4)}$ the Eq. (12b) is transformed into

$$(\lambda + a_3) (\lambda^2 - a_2) = 0$$

with solutions $\lambda_1 = -a_3$, $\lambda_{2,3} = \pm\sqrt{a_2}i$

$$\begin{aligned} \dot{\lambda} &= \frac{\frac{1}{2}(a_1^2 + 4a_2a_4)^{-\frac{1}{2}}(2a_1)}{3\lambda^2 + 2a_3\lambda + a_2} \\ \Rightarrow \dot{\lambda}(a_C) &= \frac{a_1(a_1^2 + 4a_2a_4)^{-\frac{1}{2}}}{3\lambda^2 + 2a_3\lambda + a_2} \Bigg|_{a_1=\sqrt{a_2(a_2a_3^2-4a_4)}}. \end{aligned} \quad (15)$$

Inserting $\lambda_{2,3} = \pm\sqrt{a_2}i$ in Eq. (15), the real and imaginary parts are given in Eq. (16) and Eq. (17), respectively as:

$$\operatorname{Re}(\dot{\lambda}(a_C)) = \frac{-2a_1a_2}{\sqrt{a_1^2 + 4a_2a_4}(4a_2^2 + 4a_2a_3^2)} \neq 0, \quad (16)$$

$$\operatorname{Im}(\dot{\lambda}(a_C)) = \frac{-2a_3\sqrt{a_2}}{\sqrt{a_1^2 + 4a_2a_4}(4a_2^2 + 4a_2a_3^2)} \neq 0. \quad (17)$$

Consequently, the new system (7) presents a Hopf bifurcation at E_2 .

Obviously, Eq. (14) (Critical Value) can be written in another way as

$$a_3 = \frac{a_1^2 + 4a_2a_4}{a_2\sqrt{a_1^2 + 4a_2a_4}} = a_C. \quad (18)$$

Herein $a_C = 12.6491$ under typical $(a_1, a_2, a_4) = (3, 0.25, 1)$. According to the critical value and the control parameter a_3 , the proposed system can produce three categories of point E_2 : saddle-foci (unstable), non-hyperbolic (bifurcation), and node-foci (stable), Table 2 illustrates these categories with variation a_3 .

Table 2: Classification of equilibrium point E_2 based on critical value ($a_C = 12.6491$) with parameters $(a_1, a_2, a_4) = (3, 0.25, 1)$ and varying a_3

Parameter a_3	Eigenvalues	Equilibrium E_2
$a_3 = 11.5$	$(0.001 \pm 0.5243i, -11.5022)$	Saddle-foci
$a_3 = 12.6491$	$(0.00 \pm 0.5i, -12.6491)$	Non-hyperbolic
$a_3 = 15$	$(-0.0013 \pm 0.4592i, -14.9974)$	Node-foci

3.4. Bifurcation analysis

To characterize the dynamical behavior of the proposed system relying on the bifurcation diagram and the corresponding Lyapunov exponent spectrum of the state variable x with respect to control parameter $a_2 \in [0.27, 0.33]$ and fix the parameters $(a_1, a_3, a_4) = (3, 10, 0)$. Fig. 3 exhibits various dynamical behaviors, including chaotic, periodic, and quasi-periodic.

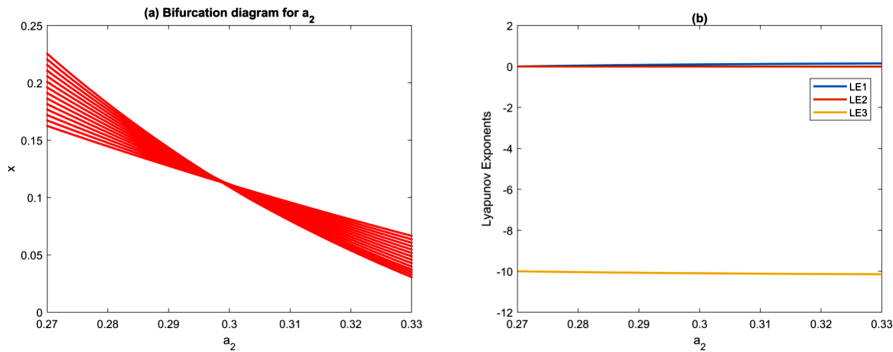


Figure 3: Bifurcation diagram and Lyapunov spectrum at $(a_1, a_3, a_4) = (3, 10, 0)$ and $a_2 \in [0.27, 0.33]$

According to Fig. 3a, the interval $[0.27, 0.33]$ is divided into three subintervals, which are summarized as:

- $a_2 \in [0.27, 0.29]$, there is $(+, 0, -)$ sign of LEs and the system (7) has chaotic attractors.
- $a_2 = 0.3$, there is $(0, 0, -)$ sign of LEs and the system (7) has quasi-periodic.
- $a_2 \in [0.31, 0.33]$, there is $(0, -, -)$ sign of LEs and the system (7) has periodic.

Some typical behaviors and Lyapunov exponents corresponding to special values of a_2 are illustrated in Fig. 4 and Table 3, respectively.

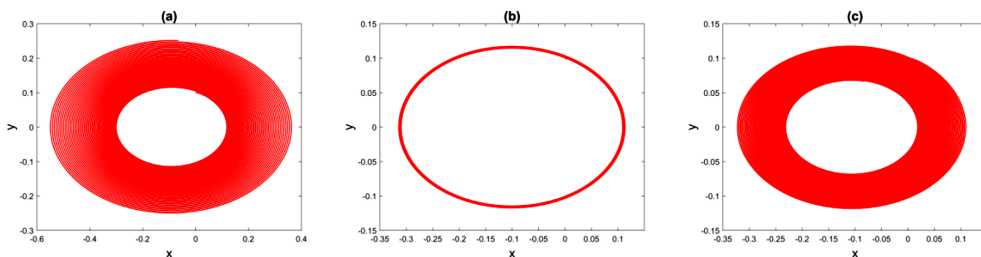


Figure 4: Typical dynamical behavior of the new system with control parameters $(a_1, a_3, a_4) = (3, 10, 0)$ and various of a_2 . (a) $a_2 = 0.27$, (b) $a_2 = 0.30$, (c) $a_2 = 0.32$

Table 3: LEs at $(a_1, a_3, a_4) = (3, 10, 0)$ with special values of a_2 and $\nabla V = -10$

Parameters a_2	Lyapunov exponent	Sum of LEs	sign of LEs	Behavior	Figure
0.27	$LE_1 = 0.0023$ $LE_2 = \mathbf{0.0006}$ $LE_3 = -10.0028$	-9.9999	$(+, \mathbf{0}, -)$	Chaotic	Fig. 4a
0.3	$LE_1 = \mathbf{0.0009}$ $LE_2 = -\mathbf{0.0009}$ $LE_3 = -9.9998$	-9.9998	$(\mathbf{0}, \mathbf{0}, -)$	Quasi-periodic (2 torus)	Fig. 4b
0.32	$LE_1 = \mathbf{0.0000}$ $LE_2 = -0.0019$ $LE_3 = -9.9979$	-9.9998	$(\mathbf{0}, -, -)$	Periodic	Fig. 4c

3.5. Influence of parameters

The parameters of the proposed system $a_i, i = 1, \dots, 4$ are called control parameters effect on the dynamical behavior of this system as shown in Fig. 5.

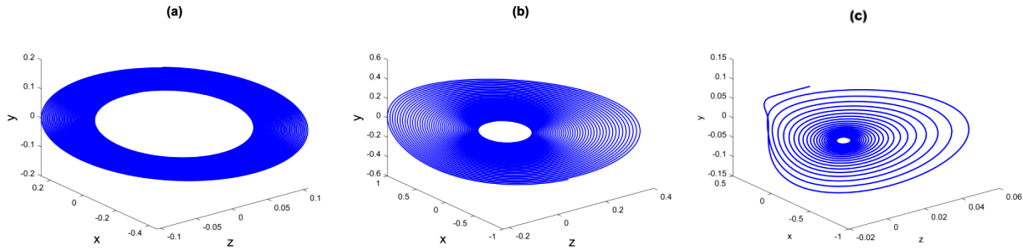


Figure 5: The attractor of the new system with various control parameters (a_1, a_2, a_3, a_4) at: (a) $(3, 0.28, 10, 0)$, (b) $(3, 0.25, 10, 1)$, (c) $(0, 0.19, 10, 1)$

- With $(a_1, a_2, a_3, a_4) = (3, 0.28, 10, 0)$, the new system without equilibria points and generates a hidden chaotic attractor as shown in Fig. 5a under the initial conditions $(0, 0.1, 0)$, the corresponding Lyapunov exponents and Lyapunov dimension are illustrated in Table 4.
- With $(a_1, a_2, a_3, a_4) = (3, 0.25, 10, 1)$, system (7) has two unstable equilibria points $P_{1,2} \left(\frac{3}{2} \pm \frac{\sqrt{10}}{2}, 0, 0 \right)$ saddle/saddle-foci and system (7) generate another typical self-excited chaotic attractor as shown in Fig. 5b and the correspond eigenvalues, Lyapunov exponents and Lyapunov dimension are given in Table 4.

- With $(a_1, a_2, a_3, a_4) = (0, 0.19, 10, 1)$, the system (7) has two stable and unstable equilibria points $P_{1,2}(\pm\sqrt{0.19}, 0, 0)$ node-foci/saddle and system (7) has coexistence of multiple attractors: self-excited and hidden periodic shown in Fig. 5c, the corresponding eigenvalues, Lyapunov exponents and Lyapunov dimension are listed in Table 4.

Table 4: Several typical attractors of the system (7) with various control parameters

Parameters a_i	Equilibria	Eigenvalues	Attractor	LE _{<i>i</i>}	D_L
(3, 0.28, 10, 0)	No equilibria	...	hidden	LE ₁ = 0.0019 LE ₂ = 0.0000 LE ₃ = -10.0061	2.0001
(3, 0.25, 10, 1)	$\left(\frac{3}{2} + \frac{\sqrt{10}}{2}, 0, 0\right)$ $\left(\frac{3}{2} - \frac{\sqrt{10}}{2}, 0, 0\right)$	$\lambda_1 = 0.5361$ $\lambda_2 = -0.5932$ $\lambda_3 = -9.9429$ $\lambda_1 = -10.0066$ $\lambda_{2,3} = 0.0033 + 0.5621i$	self-excited	LE ₁ = 0.0062 LE ₂ = 0.0000 LE ₃ = -10.0061	2.0006
(0, 0.19, 10, 1)	$(\sqrt{0.19}, 0, 0)$ $(-\sqrt{0.19}, 0, 0)$	$\lambda_1 = 0.2821$ $\lambda_2 = -0.3099$ $\lambda_3 = -9.9722$ $\lambda_1 = -9.9897$ $\lambda_{2,3} = -0.0051 + 0.2954i$	multiple attractors	LE ₁ = 0.0002 LE ₂ = -0.0115 LE ₃ = -9.9881	1.0174

4. The proposed algorithm

Data encryption plays a crucial role in maintaining information confidentiality, particularly when sensitive data is transmitted over unsecured channels. Considering this, our proposed system for image encryption serves as evidence of the potential of utilizing such systems for enhancing security and confidentiality in various applications.

A new algorithm for image encryption has been developed that employs a 3-D jerk chaotic system for encrypting colored images. The encryption process begins by detecting the original-colored image, which is then encrypted using our following proposed algorithm as depicted in Fig. 6. The original image has dimensions of $h \times w$.

Following the completion of all the necessary procedures and acquisition of the outcomes, statistical tests utilizing mathematical approaches were employed to evaluate the results. Efficiency measures, including Mean Squared Error (MSE), are used to assess the level of misrepresentation in the image, the correlation coefficient used to evaluate the association between variables, and PSNR (Peak Signal-to-Noise Ratio) which measures the quality of the encrypted image by

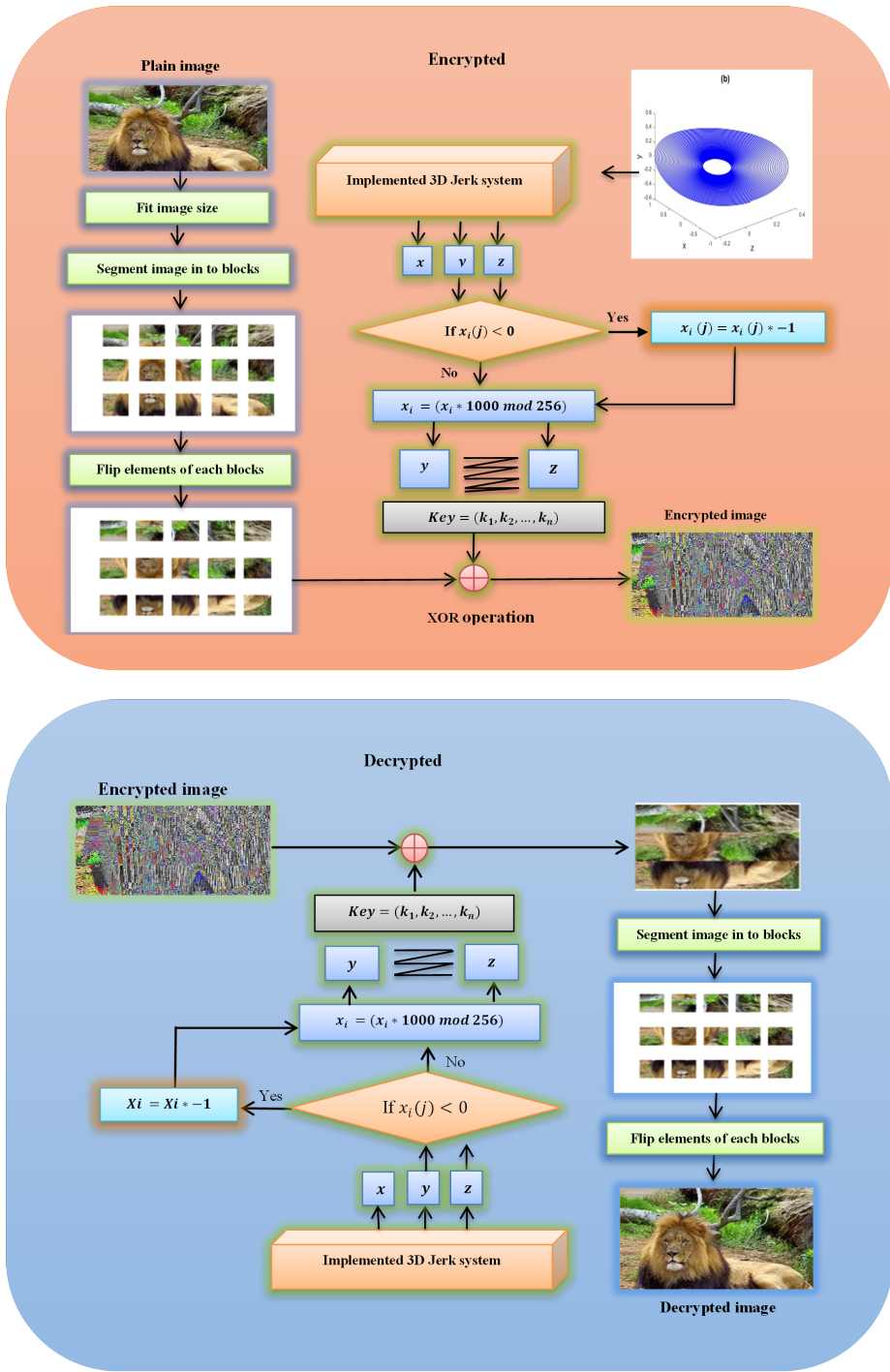


Figure 6: Block diagram of image encryption and image description process

The proposed Algorithm: Image encryption algorithm

1. Resize the image to fit the process of cutting into blocks,
 2. Divide the image into a group of blocks, each block is 50 * 50,
 3. Flipping the elements of each block to increase security,
 4. Implementation of the 3D jerk system which produces three state variables xyz ,
 5. Process the elements of each of the three variables, first, make all values positive, where
if $x_i(j) < 0$
Then $x_i(j) = x_i(j) * -1$
Else $x_i(j) = x_i(j)$,
 6. Process values greater than 255 where if
 $x_i(j) \geq 255$
Then $x_i(j) = x_i(j) \text{ mod } 255$
Else $x_i(j) = x_i(j)$,
 7. Building a key matrix in Zack Zag style from the two variables y, z ,
 8. Carrying out the encryption process by applying the XOR operation for the flipping image blocks elements with the key matrix elements,
 9. Get the encrypted image.
-

comparing it with the plain image, were utilized during the evaluation process where

$$MSE = \frac{1}{MN} \sum_{i=1}^M \sum_{j=1}^N (x_{ij} - y_{ij})^2, \quad (19)$$

$$Corr = \frac{\sum_{i=1}^N \sum_{j=1}^M (x_{ij} - \bar{x})(y_{ij} - \bar{y})}{\sqrt{\sum_{i=1}^N \sum_{j=1}^M (x_{ij} - \bar{x})^2} \sqrt{\sum_{i=1}^N \sum_{j=1}^M (y_{ij} - \bar{y})^2}}, \quad (20)$$

where \bar{x}, \bar{y} represents the mean of images x and y and can be calculated as follows:

$$\bar{x} = \sum_{i=1}^N \sum_{j=1}^M \frac{x_{ij}}{NM}, \quad \bar{y} = \sum_{i=1}^N \sum_{j=1}^M \frac{y_{ij}}{NM} \quad (21)$$

and $PSNR$

$$PSNR = 10 \log_{10} \left(\frac{C_{\max}^2}{MSE} \right). \quad (22)$$

To achieve optimal outcomes, multiple tests were conducted. Each of the resulting system sequences was used individually during the image encoding procedure to assess the influence of linear and non-linear variables on the encoding output.

The encoder utilized the XOR function to combine the color values of image pixels with the resulting string following some preliminary processing of these strings. The statistical measures of these outcomes are presented in Fig. 7.

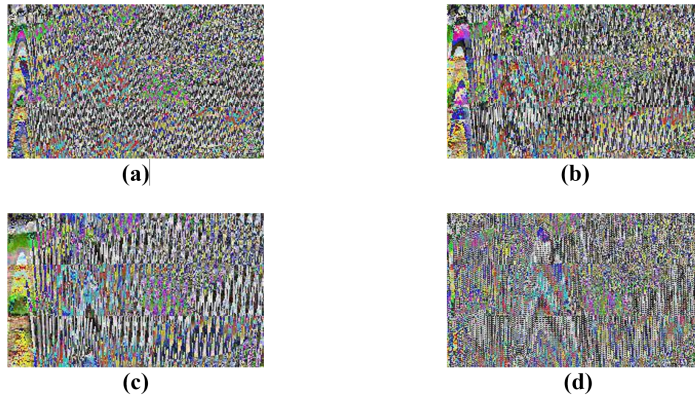


Figure 7: Encryption image with system strings results uses variables (a) x ; (b) y ; (c) z ; (d) y and z

Based on the observed outcomes, it appears evident that utilizing the first and second series obtained from the equation did not produce outcomes as satisfactory as the rest of the results. This is because the first and second equations in the system are linear, while the third equation is nonlinear. To enhance the encryption results, it was proposed to construct a keychain by combining the second and third strings, as the outcomes demonstrate. The statistical measures employed in the study are presented in Table 5.

To evaluate the effectiveness of the suggested algorithm, we utilized multiple images and began the merging and configuration process using the string from the 5000th site. We measured the algorithm's performance using Mean Squared Error, correlation, and Peak Signal-to-Noise Ratio on five images utilizing both y and z . Through statistical testing, we compared the original images with the

Table 5: MSE, Corr, and Peak-SNR between the original image and encrypted Image uses x , y , z and y and z

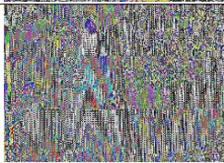
Peak-SNR	Corr	MSE	Variables
10.25073	0.01968	97.09727	x
10.43436	0.04557	102.24683	y
10.50899	-0.00988	92.78875	z
10.47239	0.01129	96.64012	y and z

encrypted and decrypted images, and the results were presented in Tables 6 and 7, demonstrating the accuracy of the algorithm.

Table 6: Statistical measures between the original image and encrypted image and the original image and decrypted image use y and z

Images	Original and encrypted images			Original and decrypted images		
	MSE	Corr	Peak-SNR	MSE	Corr	Peak-SNR
1	83.63747	0.00019	8.22620	19.79072	0.99477	31.54938
2	75.30725	0.00317	8.92621	27.84417	0.98813	29.64523
3	96.64012	0.01129	10.472398	8.72718	0.99450	35.60986
4	104.67066	0.00061	8.88281	19.66175	0.99481	31.80955
5	74.81339	0.00018	7.45140	11.74053	0.99765	34.27360

Table 7: Experimental results of the encryption algorithm using the matrix obtained from merging y and z start merging from position 5000

	Plain image	Encrypted image	Decrypted image
1			
2			
3			
4			
5			

From the practical experiments and comparison between the original image and the encrypted image, the values of metrics mean squared error (MSE), Correlation, and Peak signal-to-noise ratios (PSNR) are (74.81339 – 104.67066), (0.00018 – 0.01129) and, (7.45140 – 10.472398), respectively. Whereas the values of the same metrics: MSE, Corr., and PSNR between the original images and decrypted images, are (8.72718 – 27.84417), (0.98813 – 0.99765) and (29.64523 – 35.60986), respectively as depicted in Table 5. This indicates levels of mismatch and high obscurity, with a negligible relationship between the plain and encrypted images, and the extent of distortion achieved by the encryption algorithm. Whilst the decryption process introduces a simple level of distortion, the strong relationship between the two sets of images means a high degree of similarity between the original and decrypted images. The Peak-SNR values for the original and decrypted images are generally high, suggesting that the decryption process maintains image quality.

5. Conclusions

In this article, a new 3D jerk system is developed using a chaotic model memory oscillator (MO_4) with four adjustable parameters. By choosing the appropriate parameter, the system can exhibit different types of behavior and attractors, such as dissipative or conservative behavior, and self-excited or hidden attractors. Several characteristics are obtained from the equilibrium under specified parameters included saddle-foci, non-hyperbolic, and node-foci. The proposed system exhibits various behavior: chaotic, quasi-periodic (2-torus), and periodic attractors via utilized both software bifurcation diagrams and Lyapunov spectrum analysis. Finally this system is employed in application of images encryption and decryption which indicates its practical benefit.

References

- [1] E.N. LORENZ: Deterministic nonperiodic flow. *Journal of Atmospheric Sciences*, **20**(2), (1963), 130–141, DOI: [10.1175/1520-0469\(1963\)020<0130:DNF>2.0.CO;2](https://doi.org/10.1175/1520-0469(1963)020<0130:DNF>2.0.CO;2)
- [2] S.F. AL-AZZAWI, M.A. MOHAMED, H. RUBIANI, M. MAMAT, J. TITALEY and Y.A.R. LANG: Chaotic Lorenz system and its suppressed. *Journal of Advanced Research in Dynamical and Control*, **12**(2), (2020), 548–555, DOI: [10.5373/JARDCS/V12I2/S20201076](https://doi.org/10.5373/JARDCS/V12I2/S20201076)
- [3] J.C. SPROTT: Some simple chaotic flows. *Physical Review E*, **50**(2), (1994), R647, DOI: [10.1103/PhysRevE.50.R647](https://doi.org/10.1103/PhysRevE.50.R647)
- [4] M. MOLAIE, S. JAFARI, J.C. SPROTT and S.M.R.H. GOLPAYEGANI: Simple chaotic flows with one stable equilibrium. *International Journal of Bifurcation and Chaos*, **23**(1), (2013), 1350188, DOI: [10.1142/S0218127413501885](https://doi.org/10.1142/S0218127413501885)
- [5] J.C. SPROTT: *Elegant chaos: algebraically simple chaotic flows*. World Scientific, 2010.

- [6] F. YU, W. ZHANG, X. XIAO, W. YAO, S. CAI, J. ZHANG and Y. LI: Dynamic analysis and FPGA implementation of a new, simple 5D memristive hyperchaotic Sprott-C system. *Mathematics*, **11**(3), (2023), DOI: [701.10.3390/math11030701](https://doi.org/10.10390/math11030701)
- [7] S.F. AL-AZZAWI and A.S. AL-OBEIDI: Chaos synchronization in a new 6D hyperchaotic system with self-excited attractors and seventeen terms. *Asian-European Journal of Mathematics*, **14**(5), (2021), 2150085, DOI: [10.1142/S1793557121500856](https://doi.org/10.1142/S1793557121500856)
- [8] Q. LAI and S. CHEN: Generating multiple chaotic attractors from Sprott B system. *International Journal of Bifurcation and Chaos*, **26**(11), (2016), 1650177, DOI: [10.1142/S0218127416501777](https://doi.org/10.1142/S0218127416501777)
- [9] H. JIA, W. SHI, L. WANG and G. QI: Energy analysis of Sprott-A system and generation of a new Hamiltonian conservative chaotic system with coexisting hidden attractors. *Chaos, Solitons & Fractals*, **133**, (2020), 109635, DOI: [10.1016/j.chaos.2020.109635](https://doi.org/10.1016/j.chaos.2020.109635)
- [10] M. A. AL-HAYALI and F.S. AL-AZZAWI: A 4D hyperchaotic Sprott S system with multi-stability and hidden attractors. *Journal of Physics: Conference Series*. **1879**(3), (2021), 032031, DOI: [10.1088/1742-6596/1879/3/032031](https://doi.org/10.1088/1742-6596/1879/3/032031)
- [11] S.F. AL-AZZAWI and M.A. AL-HAYALI: Coexisting of self-excited and hidden attractors in a new 4D hyperchaotic Sprott-S system with a single equilibrium point. *Archives of Control Sciences*, **32**(1), (2022), 37–56, DOI: [10.24425/acs.2022.140863](https://doi.org/10.24425/acs.2022.140863)
- [12] O.S. OJONIYI and A.N. NJAH: A 5D hyperchaotic Sprott B system with coexisting hidden attractors. *Chaos, Solitons and Fractals*, **87**, (2016), 172–181, DOI: [10.1016/j.chaos.2016.04.004](https://doi.org/10.1016/j.chaos.2016.04.004)
- [13] S.F. AL-AZZAWI and M.A. AL-HAYALI: Multiple attractors in a novel simple 4D hyperchaotic system with chaotic 2-torus and its circuit implementation. *Indian Journal of Physics*, **97**(4), (2023), 1169–1179, DOI: [10.1007/s12648-022-02483-0](https://doi.org/10.1007/s12648-022-02483-0)
- [14] Q. YANG and C. CHEN: A 5D hyperchaotic system with three positive Lyapunov exponents coined. *International Journal of Bifurcation and Chaos*, **23**(6), (2013), 1350109, DOI: [10.1142/S0218127413501095](https://doi.org/10.1142/S0218127413501095)
- [15] Q. YANG, W.M. OSMAN and C. CHEN: A new 6D hyperchaotic system with four positive Lyapunov exponents coined. *International Journal of Bifurcation and Chaos*, **25**(4), (2015), 1550060, DOI: [10.1142/S0218127415500601](https://doi.org/10.1142/S0218127415500601)
- [16] Q. YANG, D. ZHU and L. YANG: A new 7D hyperchaotic system with five positive Lyapunov exponents coined. *International Journal of Bifurcation and Chaos*, **28**(5), (2018), 1850057, DOI: [10.1142/S0218127418500578](https://doi.org/10.1142/S0218127418500578)
- [17] J.C. SPROTT: A new class of chaotic circuit. *Physics Letters A*, **266**(1), (2000), 19–23, DOI: [10.1016/S0375-9601\(00\)00026-8](https://doi.org/10.1016/S0375-9601(00)00026-8)
- [18] S. VAIDYANATHAN, K. BENKOUIDER, A. SAMBAS and S.A. SAFAAN: A new 4-D hyperchaotic four-wing system, its bifurcation analysis, complete synchronization and circuit simulation. *Archives of Control Sciences*, **32**(3), (2022), 507–534, DOI: [10.24425/acs.2022.142847](https://doi.org/10.24425/acs.2022.142847)
- [19] S. VAIDYANATHAN, K. BENKOUIDER, A. SAMBAS and P. DARWIN: Bifurcation analysis, circuit design and sliding mode control of a new multistable chaotic population model with

- one prey and two predators. *Archives of Control Sciences*, **33**(1), (2023), 127—153, DOI: [10.24425/acs.2023.145117](https://doi.org/10.24425/acs.2023.145117)
- [20] N. HADJ TAIEB, M.A. HAMMAMI and F. DELMOTTE: Stability analysis and design of state estimated controller for delay fuzzy systems with parameter. *Archives of Control Sciences*, **32**(4), (2022), 709–731, DOI: [10.24425/acs.2022.143668](https://doi.org/10.24425/acs.2022.143668)
- [21] J.C. SPROTT: A proposed standard for the publication of new chaotic systems. *International Journal of Bifurcation and Chaos*, **21**(9), (2011), 2391–2394, DOI: [10.1142/S021812741103009X](https://doi.org/10.1142/S021812741103009X)
- [22] S. VAIDYANATHAN, C.K. VOLOS, I.M. KYPRIANIDIS, I.N. STOUBOULOS and V.T. PHAM: Analysis, adaptive control and anti-synchronization of a six-term novel jerk chaotic system with two exponential nonlinearities and its circuit simulation. *Journal of Engineering Science and Technology Review*, **8**(2), (2015), 24–36, DOI: [10.25103/jestr.082.05](https://doi.org/10.25103/jestr.082.05)
- [23] S. VAIDYANATHAN, A. SAMBAS, M. MAMAT and W.S. MADA SANJAYA: Analysis, synchronisation and circuit implementation of a novel jerk chaotic system and its application for voice encryption. *International Journal of Modelling, Identification and Control*, **28**(2), (2017), 153–166, DOI: [10.1504/IJMIC.2017.10006361](https://doi.org/10.1504/IJMIC.2017.10006361)
- [24] S.A. FADHEL, Z.N. AL-KATEEB and M.J. AL-SHAMDEEN: An improved data hiding using pixel value difference method and hyperchaotic system. *Journal of Physics: Conference Series*, **1879**(2), (2021), 022089, DOI: [10.1088/1742-6596/1879/2/022089](https://doi.org/10.1088/1742-6596/1879/2/022089)
- [25] N.M. MOHAMMED and Z.N. AL-KATEEB: A new secure encryption algorithm based on RC4 cipher and 4D hyperchaotic Sprott-S system. In *2022 Fifth College of Science International Conference of Recent Trends in Information Technology (CSCTIT)*, 131–136, IEEE, DOI: [10.1109/CSCTIT56299.2022.10145711](https://doi.org/10.1109/CSCTIT56299.2022.10145711)
- [26] A. RASLAN and A. ENTESAR: Enhancing Banach’s contraction method using the particle swarm optimization to solve the system Drinfeld-Sokolov-Wilson. *Journal of Physics: Conference Series*, **2322**(1), (2022), 012031, DOI: [10.1088/1742-6596/2322/1/012031](https://doi.org/10.1088/1742-6596/2322/1/012031)
- [27] A.N. NEGOU and J. KENGNE: Dynamic analysis of a unique jerk system with a smoothly adjustable symmetry and nonlinearity: Reversals of period doubling, offset boosting and coexisting bifurcations. *AEU-International Journal of Electronics and Communications*, **90**, (2018), 1–19, DOI: [10.1016/j.aeue.2018.04.003](https://doi.org/10.1016/j.aeue.2018.04.003)
- [28] K. RAJAGOPAL, V.T. PHAM, F.R. TAHIR, A. AKGUL, H.R. ABDOLMOHAMMADI and S. JAFARI: A chaotic jerk system with non-hyperbolic equilibrium: Dynamics, effect of time delay and circuit realisation. *Pramana*, **90**(52), (2018), 1–8, DOI: [10.1007/s12043-018-1545-x](https://doi.org/10.1007/s12043-018-1545-x)
- [29] W. FENG, Y.G. HE, C.L. LI, X.M. SU and X.Q. CHEN: Dynamical behavior of a 3D jerk system with a generalized Memristive device. *Complexity*, **2018**, (2018), DOI: [10.1155/2018/5620956](https://doi.org/10.1155/2018/5620956)
- [30] J.R.M. PONE, S.T. KINGNI, G.R. KOL and V.T. PHAM: Hopf bifurcation, antimonotonicity and amplitude controls in the chaotic Toda jerk oscillator: analysis, circuit realization and combination synchronization in its fractional-order form. *Journal for Control, Measurement, Electronics, Computing and Communications*, **60**(2), (2019), 149–161, DOI: [10.1080/00051144.2019.1600109](https://doi.org/10.1080/00051144.2019.1600109)

- [31] S. ZHANG and Y. ZENG: A simple jerk-like system without equilibrium: Asymmetric coexisting hidden attractors, bursting oscillation and double full Feigenbaum remerging trees. *Chaos, Solitons and Fractals*, **120**, (2019), 25–40, DOI: [10.1016/j.chaos.2018.12.036](https://doi.org/10.1016/j.chaos.2018.12.036)
- [32] K. LAMAMRA, S. VAIDYANATHAN, W.T. PUTRA, E. DARNILA and A. SAMBAS: A new 3-D chaotic jerk system with four nonlinear terms, its backstepping synchronization and circuit simulation. *Journal of Physics: Conference Series*, **1477**(2), (2020), 022017, DOI: [10.1088/1742-6596/1477/2/022017](https://doi.org/10.1088/1742-6596/1477/2/022017)
- [33] L.K. KENGNE, H.K. TAGNE, J.M. PONE and J. KENGNE: Dynamics, control and symmetry-breaking aspects of a new chaotic jerk system and its circuit implementation. *The European Physical Journal Plus*, **135**(3), (2020), 340, DOI: [10.1140/epjp/s13360-020-00338-3](https://doi.org/10.1140/epjp/s13360-020-00338-3)
- [34] M. JOSHI and A. RANJAN: An autonomous simple chaotic jerk system with stable and unstable equilibria using reverse sine hyperbolic functions. *International Journal of Bifurcation and Chaos*, **30**(5), (2020), 2050070, DOI: [10.1142/S0218127420500704](https://doi.org/10.1142/S0218127420500704)
- [35] K. RAJAGOPAL, S.T. KINGNI, G.H. KOM, V.T. PHAM, A. KARTHIKEYAN and S. JAFARI: Self-excited and hidden attractors in a simple chaotic jerk system and in its time-delayed form: analysis, electronic implementation, and synchronization. *Journal of the Korean Physical Society*, **77**(2), (2020), 145–152, DOI: [10.3938/jkps.77.145](https://doi.org/10.3938/jkps.77.145)
- [36] C. LI, J.C. SPOTT, W. JOO-CHEN THIO and Z. GU: A simple memristive jerk system. *IET Circuits, Devices & Systems*, **15**(4), (2021), 388–392, DOI: [10.1049/cds2.12035](https://doi.org/10.1049/cds2.12035)
- [37] M.H. ARSHAD, M. KASSAS, A.E. HUSSEIN and M.A. ABIDO: A simple technique for studying chaos using jerk equation with discrete time sine map. *Applied Sciences*, **11**(1), (2021), 437, DOI: [10.3390/app11010437](https://doi.org/10.3390/app11010437)
- [38] M. LIU, B. SANG, N. WANG and I. AHMAD: Chaotic dynamics by some quadratic jerk systems. *Axioms*, **10**(3), (2021), 227, DOI: [10.3390/axioms10030227](https://doi.org/10.3390/axioms10030227)
- [39] A. SAMBAS, S. VAIDYANATHAN, I. MOROZ, B. IDOWU, M.A. MOHAMED, M. MAMAT and W.M. SANJAYA: A simple multi-stable chaotic jerk system with two saddle-foci equilibrium points: analysis, synchronization via active backstepping control and electronic circuit design. *International Journal of Electrical and Computer Engineering*, **11**(4), (2021), 2941–2952, DOI: [10.11591/ijece.v11i4.pp2941-2952](https://doi.org/10.11591/ijece.v11i4.pp2941-2952)
- [40] P.P. SINGH and B.K. ROY: Pliers shaped coexisting bifurcation behaviors in a simple jerk chaotic system in comparison with 21 reported systems. *IFAC-PapersOnLine*, **55**(1), (2022), 920–926, DOI: [10.1016/j.ifacol.2022.04.151](https://doi.org/10.1016/j.ifacol.2022.04.151)
- [41] X. HU, B. SANG and N. WANG: The chaotic mechanisms in some jerk systems. *AIMS Mathematics*, **7**(9), (2022), 15714–15740, DOI: [10.3934/math.2022861](https://doi.org/10.3934/math.2022861)
- [42] P.C. RECH: Self-excited and hidden attractors in a multistable jerk system. *Chaos, Solitons and Fractals*, **164**, (2022), 112614, DOI: [10.1016/j.chaos.2022.112614](https://doi.org/10.1016/j.chaos.2022.112614)
- [43] S. VAIDYANATHAN, K. BENKOUIDER and A. SAMBAS: A new multistable jerk chaotic system, its bifurcation analysis, backstepping control-based synchronization design and circuit simulation. *Archives of Control Sciences*, **32**(1), (2022), 123–152, DOI: [10.24425/acs.2022.140868](https://doi.org/10.24425/acs.2022.140868)

- [44] R. SURESH, K. SATHISH KUMAR, M. REGAN, K.A. NIRANJAN KUMAR, R. NARMADA DEVI and A.J. OBAID: Dynamical properties of a modified chaotic Colpitts oscillator with triangular wave non-linearity. *Archives of Control Sciences*, **33**(1), (2023), 25–53, DOI: [10.24425/acs.2023.145112](https://doi.org/10.24425/acs.2023.145112)
- [45] N. KHAN, M.A. QURESHI, S. AKBAR and A. ARA: Probing 3D chaotic Thomas' cyclically attractor with multimedia encryption and electronic circuitry. *Archives of Control Sciences*, **33**(1), (2023) 239–271, DOI: [10.24425/acs.2023145120](https://doi.org/10.24425/acs.2023145120)
- [46] M.A. MOHAMED, T. BONNY, A. SAMBAS, S. VAIDYANATHAN, W. AL NASSAN, S. ZHANG, K. OBAIDEEN, M. MAMAT and MOHD K.M. NAWAWI: A speech cryptosystem using the new chaotic system with a capsule-shaped equilibrium curve. *Computers, Materials and Continua*, **75**(3), (2023), 5987–6006, DOI: [10.32604/cmc.2023.035668](https://doi.org/10.32604/cmc.2023.035668)